Available online at www.sciencedirect.com
SCIENCE DIRECT®
Composite Structures 67 (2005) 443–452
COMPOSITE STRUCTURES
www.elsevier.com/locate/compstruct

# Optimal design of filament wound structures under internal pressure based on the semi-geodesic path algorithm

Cheol-Ung Kim, Ji-Ho Kang, Chang-Sun Hong, Chun-Gon Kim *

*Division of Aerospace Engineering, Department of Mechanical Engineering, Korea Advanced Institute of Science and Technology (KAIST), 373-1 Guseong-dong, Yuseong-gu, Daejeon 305-701, South Korea*

Available online 25 March 2004

**Abstract**

This research aims to establish an optimal design method of filament wound structures under internal pressure. So far, most design and manufacturing of filament wound structures have been based on manufacturing experiences, and there is no established design rule. In this research, the semi-geodesic path algorithm was used to calculate possible winding patterns taking into account the windability and slippage between the fiber and the mandrel surface. In addition, finite element analyses using commercial code, ABAQUS, were performed to predict the behavior of filament wound structures. On the basis of the semi-geodesic path algorithm and the finite element analysis method, a filament wound structure was designed using the genetic algorithm.


*Keywords:* Filament winding; Semi-geodesic path; ABAQUS; Genetic algorithm

## 1. Introduction

Filament winding is a popular production technique for composite structures. In the filament winding process, a fiber bundle is placed on a rotating and removable mandrel. Consequently, it is mainly applied to manufacture axisymmetric structures. Continuous filaments are an economical and excellent form of fiber reinforcement and can be oriented to match the direction of stress loaded in a structure. Fuel tanks, oxidizer tanks, motor cases and pipes are some examples of filament wound axisymmetric structures under internal pressure.

The trajectory of the fiber path and the corresponding fiber angles cannot be chosen arbitrarily because of the stability requirement. The fiber path instability induced by fiber slippage on a mandrel surface is too complicated to be predicted because it is affected by many parameters, such as temperature, mandrel shape, fiber-resin combination, surface treatment and so on.

Finite element analyses, which can predict the deformation of filament wound structures, have been performed by many researchers. However, the results have been utilized only to understand structural characteristics of filament wound structures because some limited path equations were applied to the analyses. Even though such finite element analyses are helpful to design filament wound structures, most design and manufacturing of filament wound structures have been based on manufacturing experience and experiment. Thus, most designs are not optimized to account for filament wound structures.

Carvalho et al. [1] determined the best suited feasible angle for a given surface geometry with prevention of fiber slippage and bridging over a locally concave surface. Jones et al. [2] used the delta-axisymmetric method in order to calculate the winding pattern over the dome. Koussios et al. [3] derived the uninterrupted hoop and polar fiber path equation on cylindrical pressure vessels using non-geodesic trajectories.

Rousseau et al. [4] performed parametric studies about the influence of winding patterns on the damage behavior of filament wound structures. Beakou et al. [5] used the classical laminated theory in order to analyze the influence of variable scattering on the optimum winding angle of cylindrical composites. Kabir [6] performed a finite element analysis of composite pressure vessels having a load sharing metallic liner with a 3-D laminated shell element of the commercial FEM code,

* Corresponding author. Tel.: +82-42-869-3719; fax: +82-42-869-3710.
*E-mail address:* cgkim@kaist.ac.kr (C.-G. Kim).

0263-8223/$ - see front matter © 2004 Published by Elsevier Ltd.
doi:10.1016/j.compstruct.2004.02.003

NISA-II. Hwang et al. [7] conducted the probabilistic deformation and strength prediction for a filament wound pressure vessel of 10 inches in diameter. Park et al. [8] performed the structural analysis of the filament wound motor case considering the winding angle change through the thickness and conducted a water-pressurizing test to verify the analysis procedure.

Richard et al. [9] suggested the damage strength optimization procedure of composite cylinders using numerical analysis and the reliability-based method. Krikanov [10] used analytic equations and the graphical analysis method in order to design composite pressure vessels with higher stiffness. Tabakov [11] developed an improved genetic algorithm to optimize composite pressure vessels.

Previous research about filament wound structures are categorized into fiber path predictions, structural analyses and designs. However, there is no established design method for general filament wound structures under internal pressure satisfying given design requirements.

In this study, an optimal design method of filament wound structures under internal pressure was established. Possible winding patterns considering the windability and the slippage between fiber and mandrel surface were calculated using the semi-geodesic path algorithm. In addition, finite element analyses using commercial code, ABAQUS, were performed to predict the behavior of filament wound structures. On the basis of the semi-geodesic path algorithm and the finite element analysis method, an optimal design algorithm was suggested using the genetic algorithm and applied to a symmetric composite pressure vessel.

## 2. Semi-geodesic path algorithm

### 2.1. Formulation of semi-geodesic path algorithm

In order to perform an optimal design of filament wound structures, the prediction algorithm of possible winding patterns on an arbitrary shape is necessary. That algorithm should include two considerations.

First, the slippage between the fiber and the mandrel should be considered. Realistic pattern information is very important for an optimal design because it is directly related with the accuracy of finite element analyses. As mentioned in the introduction, in recent years several researchers derived new path equations considering fiber slippage. Second, windability should be considered. Windability means a consistent overlap of fiber bands on the mandrel towards radial and circumferential directions. Even though winding paths are calculated using prediction equations, fiber bands can be concentrated at some local parts if windability is not considered.

However, previous researches about winding patterns have not included these important considerations simultaneously or have suggested only theoretical possibilities [1–3]. In this research, a new path algorithm called the 'semi-geodesic path algorithm', which can satisfy the theoretical predictions and manufacturing considerations, is suggested.

The design of a filament wound structure consists of the design of the mandrel shape and the calculation of the fiber path. In general, the mandrel shape can be determined by imposed design requirements such as internal pressure, volume and manufacturing convenience. When the liner or mandrel surface is given without considering winding patterns, various slip conditions must be taken into account.

In this study, the semi-geodesic path equation was utilized in order to describe the realistic winding pattern on general filament wound structures [12].

$$\frac{d\alpha}{dx} = \frac{\lambda(A^2 \sin^2\alpha - rr'' \cos^2\alpha) - r'A^2 \sin\alpha}{rA^2 \cos\alpha}$$
$$\text{where} \quad |\lambda| = \left|\frac{f_b}{f_n}\right| \leqslant |\mu|, \; A = \sqrt{1 + r'^2} \tag{1}$$

Eq. (1) is defined on an arbitrary surface where $\alpha$, $x$, $\theta$, $r$, $\lambda$ are the winding angle, the axial coordinate parameter, the circumferential coordinate parameter, the radial coordinate parameter and the slippage tendency between the fiber and the mandrel (Fig. 1). And more detailed derivation is shown in Ref. [12].

By integrating Eq. (1) with a known value, the winding angle can be calculated for the entire mandrel surface. There are two assumptions in the calculation of the thickness: the fiber volume fraction is maintained consistently and the number of fibers in a cross-section is always constant. With these assumptions, the thick-

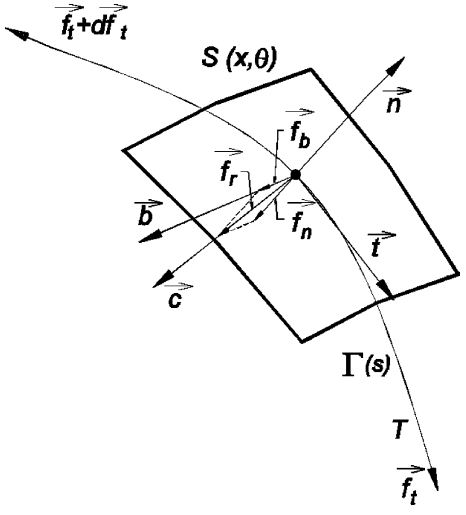


Fig. 1. Geometry of fiber path on the surface.

ness along the longitudinal direction can be derived as follows:

$$t = \frac{n_p w t_c}{2\pi r \cos\alpha} = \frac{\frac{2\pi r_c \cos\alpha_c}{w} w t_c}{2\pi r \cos\alpha} = \frac{r_c \cos\alpha_c}{r \cos\alpha} \times t_c \quad (2)$$

where $r_c$, $\alpha_c$, $t_c$, $n_p$, $w$ are radius, winding angle, thickness, number of fiber bands in a layer, and band width, respectively.

As mentioned above, windability is very important because some of the patterns calculated by Eq. (1) may be useless for the manufacture of filament wound structures unless uniform coverage is considered. The concept of windability was presented concurrently by Lossie [13] and Lowery [14]. Though notations used in the two studies are different, fundamental concepts are identical. A series of two consecutive fiber paths is called a winding circuit. The first fiber path crosses the mandrel from one end to the other end, and the second fiber path returns to the first end. The next circuit is identical to the first but shifted over the circumference of the mandrel. If the number of fiber bands in a layer is $n_p$ and the circumferential shifted integer is $m$, the relationship of $n_p$ and $m$ should be relative prime in order to satisfy the windability.

The semi-geodesic path algorithm suggested in this study considers the fiber slippage and the windability. Fig. 2 is the flow chart of the semi-geodesic path algorithm. At the first step, several input parameters are given—shape of the mandrel, slippage tendency, band width and so on. And the range of winding patterns is calculated using Eq. (1) with upper and lower bounds of slippage tendency. At the next step, feasible winding angles satisfying the windability are selected and stored into a database. Finally, detailed winding patterns about each feasible angle stored in the database are calculated.

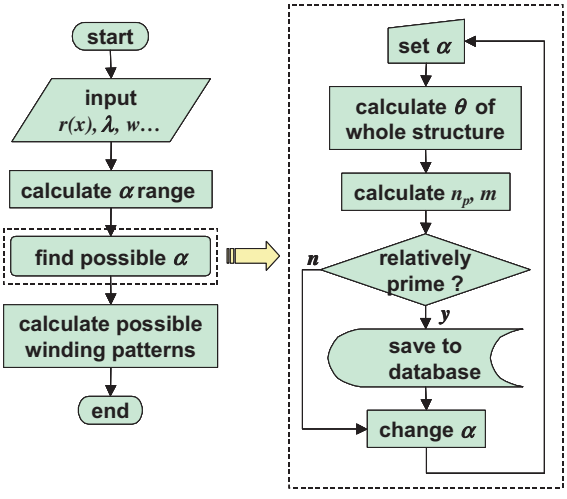


Fig. 2. Semi-geodesic path algorithm.

In this research, a graphic user interface (GUI) based program was developed using Microsoft Visual C++ to perform the semi-geodesic path algorithm (Fig. 3).

### 2.2. Applications of semi-geodesic path algorithm

#### 2.2.1. Cylinder

In order to verify the semi-geodesic path algorithm and the developed program, it was applied to a cylindrical tube (Fig. 4) which had been introduced in

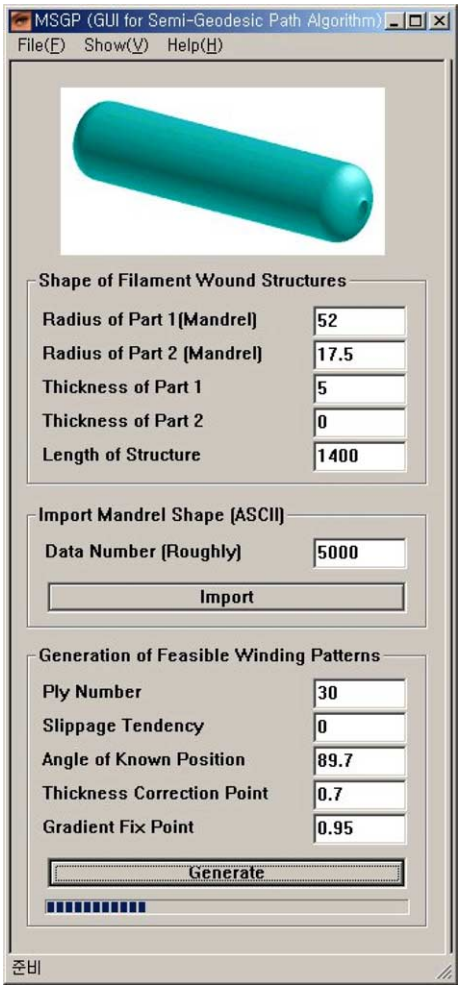


Fig. 3. Graphic user interface for the semi-geodesic path algorithm—MSGP.

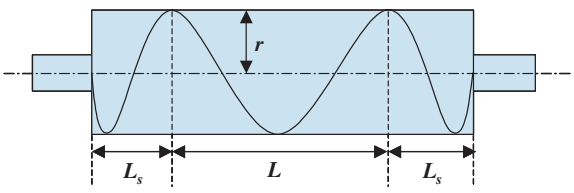


Fig. 4. Fiber path on a cylinder with return at ends.

Ref. [12]. The length of the cylinder is 1000 mm, the radius is 100 mm, the band width is 10 mm, the slippage tendency is 0.2 and the winding angle is given as 54.7°.

When the semi-geodesic path algorithm is applied to the cylinder, the minimum length of the end parts is 112.7 mm. Therefore, if the length of cylinder should be 1000 mm, a mandrel is needed with a minimum length of 1225.4 mm, 22% more than the useful length of the cylinder. In this case, the windability is satisfied because $n_p$ is 37 and $m$ is 24.

#### 2.2.2. Pressure vessel

The second application of the semi-geodesic path algorithm is a pressure vessel, and the selected model is an advanced standard test evaluation bottle (ASTEB) [15]. The ASTEB is developed to evaluate the performance of small-scale pressure vessels with respect to the design and processing parameters. It is a modified version of the STEB and has a bigger opening radius than the STEB. The radii of the cylinder, the forward dome, and the aft dome are 127, 45.8, 70.83 mm, respectively. The length of the cylinder is 454.4 mm. So, the ASTEB is an unsymmetrical tank and has isotensoid dome shapes (Fig. 5).

When the semi-geodesic path algorithm is applied to the ASTEB with 1.1 mm helical thickness, the winding angle ranges from 11.5° to 35.5° for the forward dome and form 25.5° to 47.5° for the aft dome. Therefore, the total winding angle varies form 25.5° to 35.5° because both sides are wound simultaneously as one body. If the winding angle range is divided into 0.5° step, a total of 21 winding angles can be chosen theoretically. However, some of those angles will not satisfy the windability, resulting in feasible winding angles of 25.5°, 26.5°, 27.5°, 28.0°, 28.5°, 29.5°, 31.0°, 31.5°, 32.5°, 33.0°, 33.5°, 34.0°, 34.5° and 35.5°. Hence, only 66.7% of the theoretical angles can be applied to the manufacturing of the ASTEB.

Actually, the final design angle of the ASTEB, which was drawn by manufacturing experiences and the water-pressurizing test, is 27.5°. In this case, the angle 27.5° is one of the feasible angles, and the windability is satisfied because $n_p$ is 71 and $m$ is 33.


Fig. 5. ASTEB—advanced standard test evaluation bottle.

## 3. Finite element analysis

### 3.1. Finite element modeling

So far, several types of elements have been utilized in finite element analyses of filament wound structures. However, when 2-dimensional shell elements are used in the analysis, a detailed modeling of structures is impossible without solid elements connected by rigid beams, and a stress concentration at the knuckle part is sometimes overestimated due to a rapid change in curvature and thickness. And, for an axisymmetric solid element, the 3-dimensional effective modulus should be calculated for each layer and the transformation of stress and strain towards the fiber direction should be done. As a result, the reduction of material properties in layer level is not easy in progressive failure analysis. Therefore, in recent studies, 3-dimensional(3-D) solid elements or 3-D layered solid elements are utilized [6–8]. 3-D layered solid elements used in some commercial FEM codes, are the elements adopting the layerwise theory for composites.

In this research, compared were the analysis results between the 3-D solid element and the 3-D layered solid element for the forward part of the ASTEB by a commercial code, ABAQUS. The finite element models are shown in Fig. 6. In the modeling, C3D20 type elements with 20 nodes per element were used. The two models were made in the same manner except element numbering in the thickness direction. The model using 3-D layered solid elements has 100 elements and 1113 nodes, while the model using 3-D solid elements has 500 elements and 3938 nodes. The modeling was performed for a 1.5° strip of a full tank using a cyclic symmetry boundary condition. The element size is larger at the center of the dome than that near the interface of the dome/cylinder and dome/polar opening. In the cylindrical part, 20 elements to the x-axial direction were enough to gain a converged result, but 60 elements to the meridian direction were used in the dome area. The winding path was calculated using the established semi-geodesic path algorithm. And, a preprocessor PREAFT which imposes the calculated path information on each element was developed and used (Fig. 7). The inner pressure is 13.79 MPa (2000 psi) and material properties are shown in Table 1.

The deformed shapes of the two cases are magnified 5 times and shown to be very similar regardless of the element types as shown in Fig. 8. Fig. 9 shows the fiber directional stress on the outer layer, and the two stress distributions are also similar. However, in the case of 3-D layered solid elements, the stress is

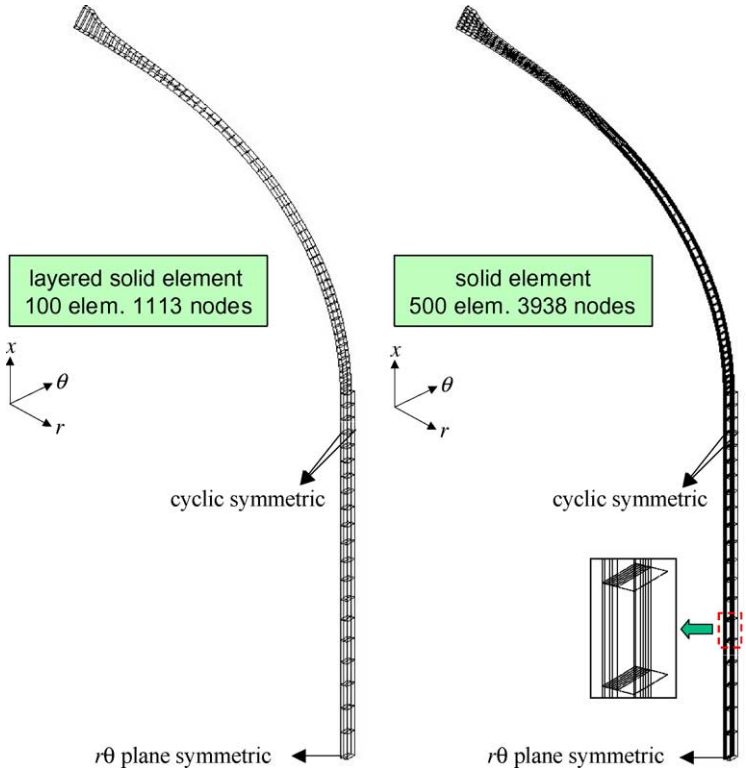


Fig. 6. Finite element models using 3-dimensional elements.

somewhat underestimated near the end of the dome because the number of elements in the thickness direction is insufficient for describing a local bending deformation.

Though the model using 3-D layered solid elements has 20% of the elements and 30% of the nodes compared to that using 3-D solid elements, results of the two analyses are reasonably similar. In general, the optimal design of composite structures must account for the reduction of time and cost. Therefore, 3-D layered solid elements are more suitable to the optimal design of filament wound structures.

### 3.2. Progressive failure analysis

In order to perform the progressive failure analysis, proper selection is needed in the failure criterion and a stiffness degradation model. So, three progressive failure analyses were performed using representative failure criteria, and the results were compared with those of an analysis considering only geometric non-linearity. Applied failure criteria are the maximum stress failure criterion, the modified Tsai-Wu failure criterion [16] and the modified Hashin's failure criterion [17]. The analysis model is the forward part of the ASTEB, and modeling details are the same as those of the previous finite element model.

For the purpose of failure analysis, a subroutine, USDFLD of ABAQUS ver 6.3 was coded to define the change of mechanical properties due to failure. An element failure is first identified and later the failed element is replaced with a degraded element. The degradation method should be carefully chosen because the results of progressive failure analyses often depend on the mesh size, degree of reduction, the increment steps, etc. The equivalent properties of the damaged element might exist between zero values and solid ones. In this study, the stiffness-reduction coefficient(SRC) varies from 0.1 to 0.9 by using Reddy's method [16]. When SRC is 0.1, the failed elements almost lose their load-carrying capacity. SRC of 0.9 means that the mechanical properties of the failed elements do not decrease much compared to those of unfailed ones. The case of SRC < 0.1 was excluded because the analysis becomes a conservative one.

Fig. 10 shows the fiber directional stresses of all cases on the outmost layer of the tank. In the case of no failure criterion, the stress level is comparatively low because the matrix crack is not considered. The stress oscillates near the junction between a dome and a cylinder, which is caused by an excessive bending deformation. However, in cases using three failure criteria, the stress levels and tendencies are very similar among each other, and a meaningful difference is not observed. Therefore, the modified Hashin's failure criterion, which is commonly used in recent studies and has many

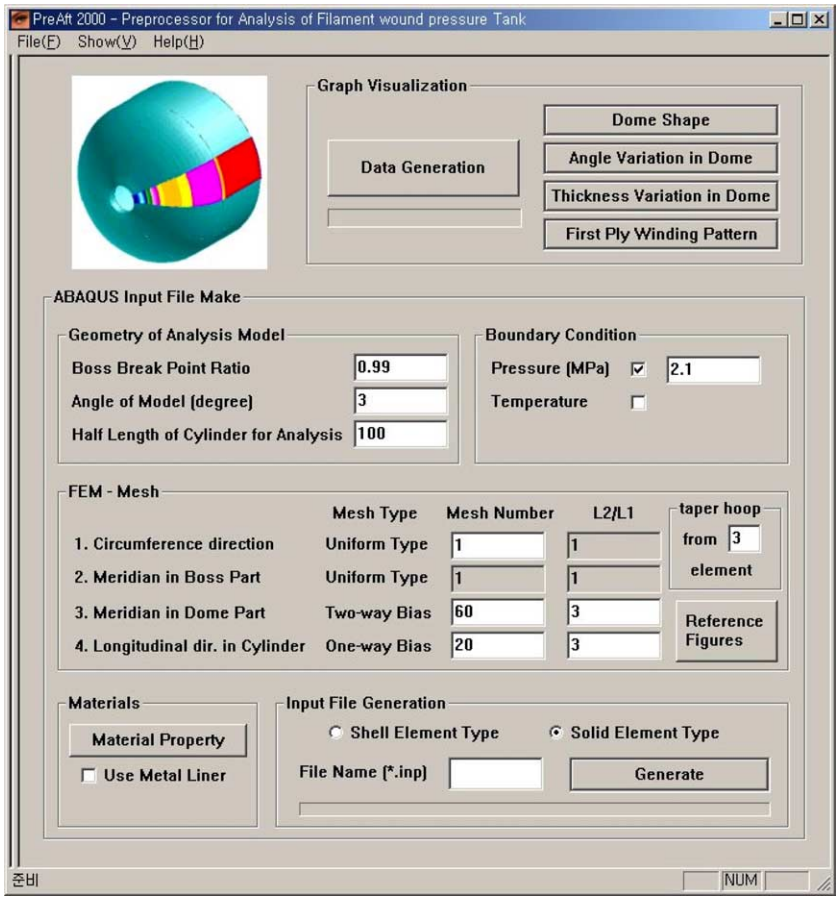


Fig. 7. Preprocessor for filament wound pressure vessels—PREAFT.

Table 1
Material property of T800/Epoxy

| | Value |
|---|---|
| $E_1$ | 161.3 GPa |
| $E_2, E_3$ | 8.820 GPa |
| $G_{12}, G_{13}$ | 5.331 GPa |
| $G_{23}$ | 2.744 GPa |
| $v_{12}, v_{13}$ | 0.33 |
| $v_{23}$ | 0.45 |
| $X_t$ | 2300 MPa |
| $X_c$ | 1080 MPa |
| $Y_t$ | 30 MPa |
| $Y_c$ | 70 MPa |
| Density, $\rho$ | $1.5\times10^{-6}$ kg/mm$^3$ |

discernable failure modes, was selected and applied to the analysis and optimal design in this research.

Fig. 11 shows the comparison of the results between the finite element analysis using the modified Hashin's failure criterion and the water-pressurizing test of our previous research [18]. It shows good agreement between them both in trend and quantity. Therefore, this analysis method is suitable for applying to the optimal design.

## 4. Optimal design using genetic algorithm

### 4.1. Genetic algorithm

Genetic algorithm [19] was used to optimize filament wound structures under internal pressure in this study. Genetic algorithm is a search algorithm based on the mechanics of natural selection and genetics. It simulates natural evolution so that multiple design points evolve to converge to a global optimum. It combines survival of the fittest among string structures having a structured yet randomized information exchange to form a search algorithm with some of the innovative flair of human search. In every generation, a new set of artificial strings is created using bits and pieces form the fittest of the old; an occasional new part is added for good measure. Its calculation process uses a non-deterministic scheme and has nothing to do with differentiability or convexity. The most useful advantage is that it uses discrete design variables by nature. Therefore, it is simple to use discrete values as design variables.

A genetic algorithm consists of three operations: function evaluation, selection and reproduction; and the two main classes of genetic operations are mutation and

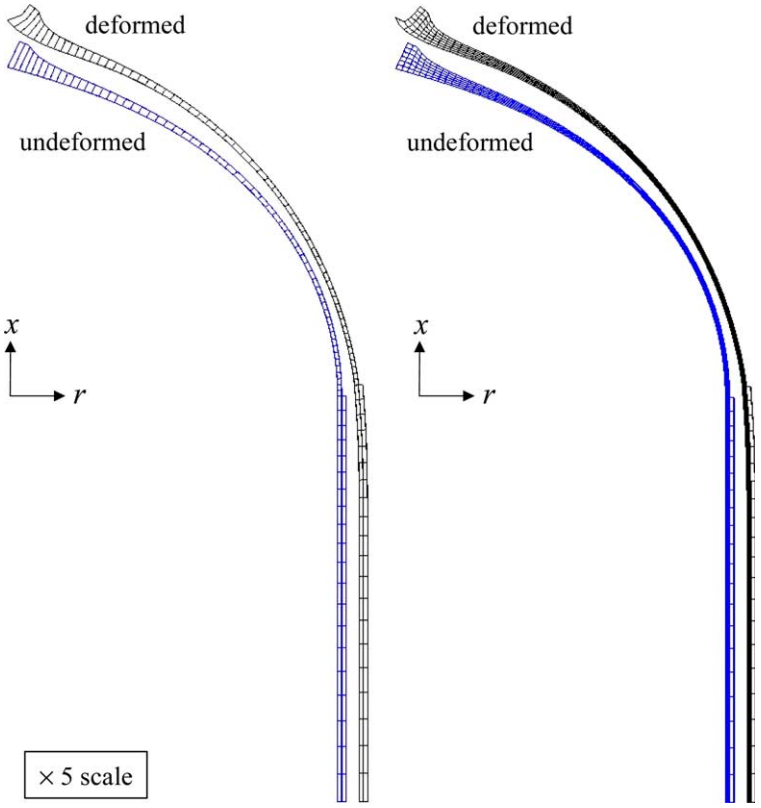


Fig. 8. Deformed shapes of ASTEB.

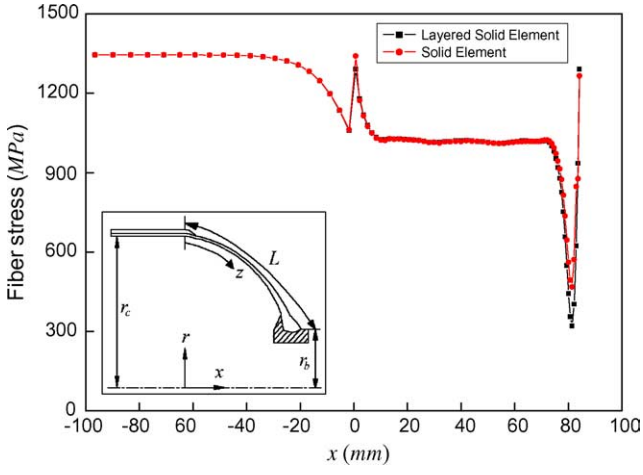


Fig. 9. Comparison of fiber stresses between layered solid element and solid element.

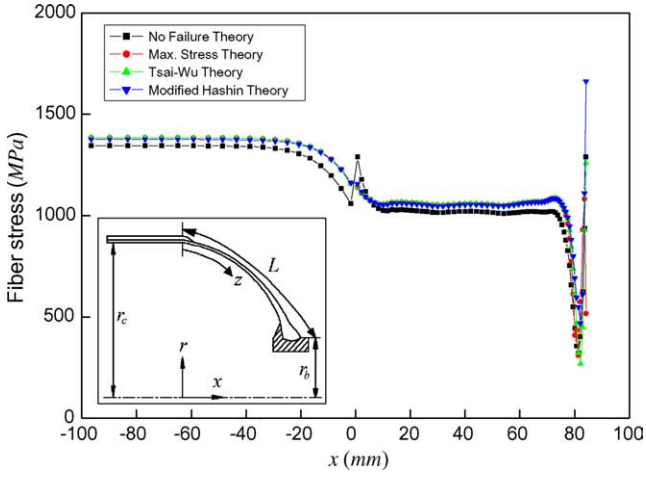


Fig. 10. FEA results using several failure theories.

crossover. Genetic algorithm is different from other optimization methods and search procedures in four ways [19]. First, it works with a coding of the parameter set, not the parameters themselves. Second, it searches from a population of points, not a single point. Third, it uses objective function, not derivatives or other auxiliary knowledge. Fourth, it uses probabilistic transition rules, not deterministic rules.

### 4.2. Design procedure

In this study, the optimal design algorithm was established, which includes the semi-geodesic path algorithm, progressive failure analysis and genetic algorithms. Fig. 12 shows the flow chart of the suggested optimal design algorithm. The genetic algorithm controls the overall procedure. The windows based program

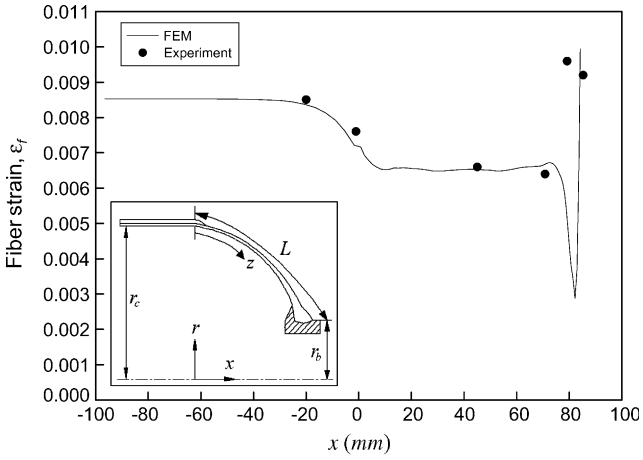


Fig. 11. Comparison of fiber strains between analysis and experiment.

for this algorithm was developed using C++ language, and it was named 'IDOTCOM_FW'.

### 4.3. Application—pressure vessel

The established optimal design algorithm was applied to a symmetric pressure tank of type 3 with a load sharing metallic liner for verification. The configuration of a tank of type 3 is shown in Fig. 13. The half shape of the tank is the same as the forward part of the ASTEB. The material of the composites is T800/Epoxy, and the liner is aluminum alloy 7075-T6.

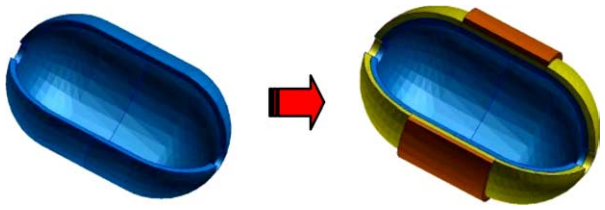

Fig. 13. The configuration of general type 3 tanks.

Basic design requirements are as follows:

1. Maximum operating inner pressure is 13.79 MPa (2000 psi).
2. The yield of the liner is not permitted.
3. The safety factor of the composite is 3.0.
4. The weight reduction is the most important goal of this design.

The objective function is defined as follows

$$f = \begin{cases} \dfrac{W_{\max}}{W} + 0.1 \times \dfrac{\sigma_{\text{f,design}}}{\sigma_{\text{fiber}}} + 0.1 \times \dfrac{\sigma_{\text{yield}}}{\sigma_{\text{liner}}}, \\ \quad \sigma_{\text{liner}} \leqslant \sigma_{\text{yield}} \text{ and } \sigma_{\text{fiber}} \leqslant \sigma_{\text{f,design}} \\ \dfrac{\sigma_{\text{f,design}}}{\sigma_{\text{fiber}}} + 0.1 \times \dfrac{\sigma_{\text{yield}}}{\sigma_{\text{liner}}}, \\ \quad \sigma_{\text{liner}} \leqslant \sigma_{\text{yield}} \text{ and } \sigma_{\text{fiber}} > \sigma_{\text{f,design}} \\ \dfrac{\sigma_{\text{yield}}}{\sigma_{\text{liner}}}, \\ \quad \sigma_{\text{liner}} > \sigma_{\text{yield}} \end{cases} \tag{3}$$

where $W_{\max}$, $W$, $\sigma_{\text{f,design}}$, $\sigma_{\text{fiber}}$, $\sigma_{\text{yield}}$, $\sigma_{\text{liner}}$ are the possible maximum weight, the weight of the design point, the

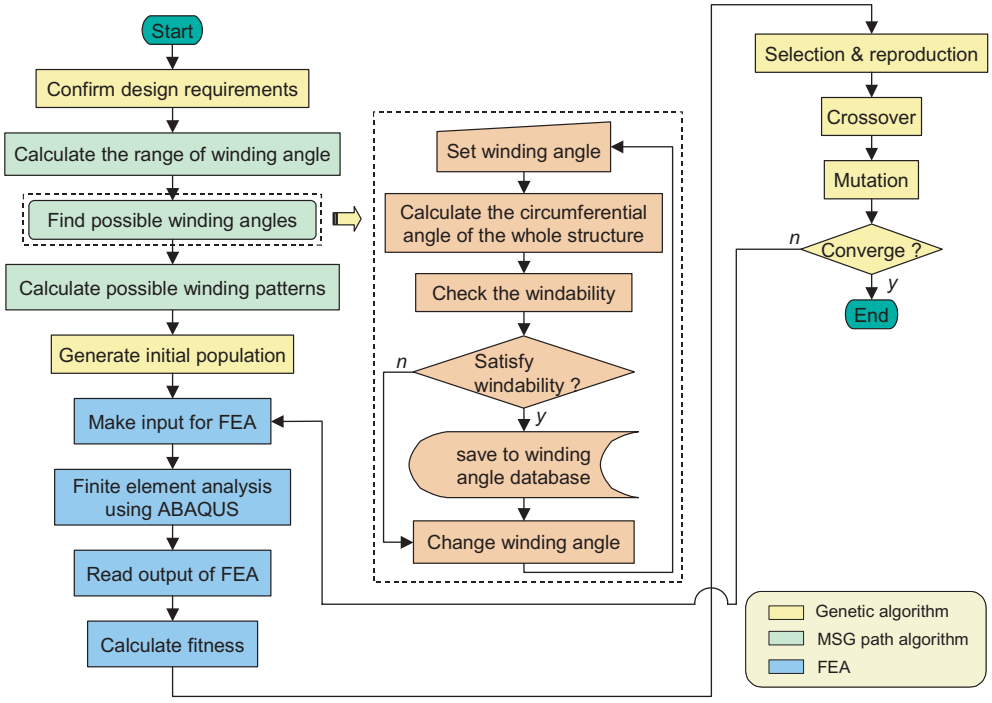


Fig. 12. Optimal design procedure for axisymmetric filament wound structures.

Table 2
Design results

| Cases | Helical layer | Hoop layer | Winding angle (°) | Liner (mm) | Weight (kg) |
|---|---|---|---|---|---|
| 1 | 2 | 9 | 33.5 | 1.9 | 4.44 |
| 2 | 3 | 10 | 34.5 | 1.7 | 4.47 |
| 3 | 2 | 9 | 31.5 | 1.9 | 4.45 |
| 4 | 3 | 10 | 28.0 | 1.7 | 4.50 |
| 5 | 2 | 10 | 33.0 | 1.9 | 4.51 |
| 6 | 2 | 9 | 33.5 | 1.9 | 4.44 |
| 7 | 2 | 9 | 33.5 | 1.9 | 4.44 |
| 8 | 3 | 10 | 33.0 | 1.7 | 4.48 |
| 9 | 3 | 9 | 34.0 | 1.8 | 4.58 |
| 10 | 2 | 9 | 31.5 | 1.9 | 4.45 |

fiber directional strength considering the safety factor, the maximum fiber directional stress of the design point, the yield strength of the liner, and the maximum von Mises stress of the liner of the design point, respectively.

The weight of the tank, the maximum fiber directional stress of the composite and the maximum stress of the liner are normalized and summed when stress terms are satisfied with maximum criteria. And, it is assumed that the relative importance of weight is ten times greater than that of stresses.

Four design variables(the number of helical layers, the number of hoop layers, the winding angle of the cylinder part, and the thickness of the liner) were set up and used in this optimal design because the goal of this application is the verification of the suggested algorithm and program. Each of them was separated to discrete values as many as 2, 4, 5 and 4 bits in order to be applied to the genetic algorithm.

From our previous researches, we determined the required parameters for genetic algorithm as follows; the population size was set as 100, the maximum number of generations as 100, the probability of crossover as 0.7, the probability of mutation as 0.1 and the tournament size for the genetic algorithm as 10. The initial seed value was generated randomly, and a total of ten optimal designs were performed.

Table 2 shows the design results. Results of seven kinds were drawn. Among them, the best case, which satisfies the given design requirements, is a tank with a weight of 4.44 kg.

## 5. Conclusion

In this research, possible winding patterns considering windability and slippage were calculated using the semi-geodesic path algorithm. In addition, progressive failure analyses were performed to predict the behavior of filament wound structures. In particular, suitable element types and failure criteria for filament wound structures were studied. In addition, on the basis of the semi-geodesic path algorithm and the finite element analysis method, an optimal design algorithm was suggested using the genetic algorithm. Finally, the developed design code was applied to a symmetric composite pressure vessel for verification.

## References

[1] De Carvalho J, Lossie M, Vandepitte D, Van Brussel H. Optimization of filament-wound parts based on non-geodesic winding. Compos Manuf 1995;6(2):79–84.
[2] Jones DT, Jones IA, Middleton V. Improving composite lay-up for non-spherical filament-wound pressure vessels. Composites: Part A 1996;27(4):311–7.
[3] Koussios S, Bergsma OK. Uninterrupted hoop-and polar-fibre paths on cylindrical pressure vessels using non-geodesic trajectories. In: American Society for Composites 17th Annual Technical Conference Proceeding CD, West Lafayette, October 2002. p. 21–3.
[4] Rousseau J, Perreux D, Verdiere N. The influence of winding patterns on the damage behaviour of filament-wound pipes. Compos Sci Technol 1999;59:1439–49.
[5] Beakou A, Mohamed A. Influence of variable scattering on the optimum winding angle of cylindrical laminated composites. Compos Struct 2001;53:287–93.
[6] Kabir MZ. Finite eelement analysis of composite pressure vessels with a load sharing metallic liner. Compos Struct 2000;49:247–55.
[7] Hwang TK, Hong CS, Kim CG. Probabilistic deformation and strength prediction for a filament wound pressure vessel. Composites: Part B 2003;34:481–97.
[8] Park JS, Kim CU, Kang HK, Hong CS, Kim CG. Structural analysis and strain monitoring of the filament wound motor case. J Compos Mater 2002;36(20):2373–88.
[9] Richard F, Perreux D. A reliability method for optimization of $[+q/-q]n$ fiber reinforced composite pipes. Reliab Eng Syst Saf 2000;68:53–9.
[10] Krikanov AA. Composite pressure vessels with higher stiffness. Compos Struct 2000;48:119–27.
[11] Tabakov PY. Multi-dimensional design optimization of laminated structures using an improved genetic algorithm. Compos Struct 2001;54:349–54.
[12] Scholliers J. Robotic filament winding of asymmetric composite parts. PhD thesis (K.U.Leuven), 1992.
[13] Lossie M. Production oriented design of filament wound composites. PhD thesis (K.U.Leuven), 1990.
[14] Lowery PA. Continued fractions and the derivation of uniform-coverage filament winding patterns. SAMPE J 1990;26:57–64.
[15] Hwang TK, Jung SK, Doh YD, Cho WM, Jung B. The performance improvement of filament wound composite pressure vessels. SAMPE 2000, 21–25 May 2000, p. 1427–38.

[16] Reddy YSN, Dakshina Moorthy CM, Reddy JN. Non-linear progressive failure analysis of laminated composite plates. Int J Non-Linear Mech 1995;30(5):629–49.
[17] Chang FK. A progressive damage model for laminated composites containing stress concentrations. J Compos Mater 1987;21:834–51.
[18] Park JS, Hong CS, Kim CG, Kim CU. Analysis of filament wound composite structures considering the change of winding angles through the thickness direction. Compos Struct 2002;55:33–71.
[19] Goldberg DE. Genetic algorithm in search, optimization, and machine learning. Addison-Wesley Publishing Company; 1989.